JOURNAL OF MECHANICS OF CONTINUA AND MATHEMATICAL SCIENCES
www.journalimcms.org

ISSN (Online) : 2454 -7190 Vol.-15, No.-8, August (2020) pp 174-187 ISSN (Print) 0973-8975

CHARACTERISTIC BEHAVIOUR OF RARE EARTH DOPED OXYFLUOROBORATE GLASSES

S. Farooq[1], V.B. Sreedhar[2], R. Padmasuvarna[3], Y. Munikrishna Reddy[4]

[1,2]Department of Physics, Rajiv Gandhi Memorial College of Engineering & Technology, Nandyal, Andhra Pradesh, India-518501

[3]Department of Physics, JNT University, Anantapuramu - 515002, India

[4]Department of Physics SSBN Degree College, Anantapuramu-51500, Andhra Pradesh, India

[1]farooqsyed2917@gmail.com, [2]vbsreedhar@gmail.com, [3]padmajntua@gmail.com, [4]ymkredi@gmail.com

Corresponding Author: **S. Farooq**

https://doi.org/10.26782/jmcms.2020.08.00016

(Received May 16, 2020; Accepted: August 3, 2020)

Abstract

A series of glasses by melt quenching method fabricated for spectroscopic investigations of Dy^{3+} ions doped Antimony (Sb)-Magnesium (Mg)-Strontium (Sr) Oxyfluoroborate (BSbMgFS) glasses. The structural and optical characterizations such as XRD, Raman, UV-visible-NIR absorption spectroscopy, photoluminescence (PL) (excitation and emission), were skilled to study the various properties of the glasses. Amorphous nature of the present glass confirm from the broad peaks of XRD. The transitions from lowestthe energy state to excited state in RE^{3+} ions were identified using optical UV-visible-NIR absorption spectra. By using Judd-Ofelt theory the J-O intensity parameters Ω_λ (λ = 2, 4, 6) have been evaluated from experimental (f_{exp}) and calculated (f_{cal}) oscillator strengths. The value of Ω_2 is higher than Ω_4 and Ω_6 and follows the trend $\Omega_2 > \Omega_6 > \Omega_4$. This confirms the high covalency of Dy^{3+} ion with ligands and more asymmetric environment around the rare earth ion in host. The emission of light from glass system was concluded through PL spectra (Excitation and emission) for Dy^{3+} ion. In the present work branching ratio of $^4F_{9/2} \rightarrow {}^6H_{13/2}$ transition is obtained higher than 50% (0.55). The highest readings of A_R, β_R and σ_{se} are obtained for the transition n $^4F_{9/2} \rightarrow {}^6H_{13/2}$ (yellow).Hence, this can be consider as an appropriate mechanism for lasing action. Gain band width ($\Delta\lambda_{eff}$ x σ_{se}) and optical-gain (σ_{se} x τ_R) were found to be high for BSbMgFSDy01 and this suggest that BSbMgFSD01 glasses were appropriate for optical amplifier. In the present study of Dy^{3+} - doped glasses, BSbMgFSD05 has shown highest emission with a Y/B ratio of 2.73 which is useful for white-LED applications. BSbMgFSDy05 glass is suitable for white light emitting devices and lasers applications in the visible region at 575 nm upon excitation of 425 nm.

Keywords : Photoluminescence, Dy^{3+} -doped glasses, Judd-Ofelt theory, PL spectra

I. Introduction

Now a day's research is growing to investigate the association, interface etc of rare earth ions with their respective host medium. The lanthanide ions doped with inorganic luminescent host materials are widely studied due to the exclusive optical properties of lanthanide ions from 4f-4f electronic transitions which support to get laser emission and optical amplification at the desired spectral range [XV, XIV, XXX, XVI , XXXVIII, XXXII, XXI,I, XXXI]. The advantages such as homogeneous light emission, better thermal stability, good chemical and mechanical strength, superior solubility of lanthanide ions, lower fabrication cost, ease of producing bulk size industrial samples, high doping capacity and uncomplicated manufacturing processes make the glasses as the promising host materials for lanthanide ions and also very superior over the phosphors [XXII, VII, XXXIV]. Glasses activated with lanthanide ions have found potential applications which includes display monitors, lasers, optical fibers, detectors, sensors, solar concentrators, color displays, optical amplifiers, light converters and solid state lighting (SSL) devices [XVII, XXIII, XIII]. In addition, the variation of concentration of lanthanide ions in host glass offers adequate room for the researchers to work on optoelectronic devices. Rare earths doped with tellurite, borate, phosphate and silicate oxide glass hosts have been recognized as suitable hosts for the advancement in the field of photonics. In various host glasses Borate glasses are of interest mainly due to low melting temperatures, compatibility with rare earth elements and transition metals, wide glass-forming range and Second- and third-order optical nonlinearity. Borate glasses are capable of vitrifying over a wide range of compositions and host rare earth oxides. Different host glasses with distinguished trivalent rare earth elements are well introduced in the literature with their properties along with the applications in various fields that include infrared amplifiers, solid state lasers, commercial filter glasses, optical communications and quantum informatics. Oxide glasses, especially silicates, have quite high phonon energy (1350 cm^{-1}) that causes non-radiative relaxation with subsequent low optical efficiency. Thereby, oxyfluoride glasses have been considered as promising host materials due to their high transparency, low melting temperature, low phonon energy and the possibility to effectively host RE ions inside the glass. Bismuth, antimony, strontium and lead based glasses are promising heavy metal oxide glasses. There is a more attention towards these glasses is due to their long infrared cut-off, optical non-linearity, high refractive index, high polarizability and low melting point.

Dy^{3+}- ions doped glasses have received great attention in development and generation of possible white light emitting devices (WLEDs). It is well known that an appropriate yellow to blue intensity ratio of the Dy^{3+} ions radiate white light. The feasibility is due to the two predominant transitions which depend on the selection of host and environment coordination. The two strong emission bands at yellow (470-500 nm) and blue (570-600 nm) regions related to the non-hypersensitive $^4F_{9/2} \rightarrow {}^6H_{3/2}$ and $^4F_{9/2} \rightarrow {}^6H_{15/2}$ transitions, respectively. Therefore, the luminescent intensity ratio

(Y/B) of above transitions can be modified in such a way that the activated Dy^{3+}-doped glasses could produce white light.

The objective of the present study is to optimize antimony-magnesium-strontium-oxyfluoroborate (BSbMgFSD) glasses as a function of Dy^{3+} ions concentration for white light luminescence. The structural and photoluminescence properties of Dy^{3+}-doped BSbMgFS glasses were examined with the aid of

- X-ray diffractometer (XRD).
- Varian Cary-5000 double beam absorption spectrometer.
- Edinburg SpectroFluorometer-950.
- The radiative properties such as transition probabilities (A_R), branching ratio β_R (β_{exp} & β_{cal}), stimulated emission cross-sections (σ_{se}), radiative lifetime τ_R (ms), gain band width ($\Delta\lambda_{eff}$ x σ_{se}) and optical-gain (σ_{se} x τ_R) were obtained from J-O intensity parameters.
- CIE 1931 diagram.

II. Experimental Techniques

II.i. Synthesis

BSbMgFSD glass matrices doped with Dy^{3+} ion were synthesized by well-known melt-quenching method with the glass composition $(70\text{-}x)B_2O_3+10MgF_2+15SrO+5Sb_2O_3+xD_2O_3$, where x =0.1, 0.5, 1.0, 1.5, 2.0 and 2.5 mol%, and tagged as BSbMgFSD01, BSbMgFSD05, BSbMgFSD10, BSbMgFSD15, BSbMgFSD20 and BSbMgFSD25 respectively. A mixture of glass composition of about 15 g was weighed using a micro balance and pulverized in an agate mortar to achieve the said composition with high homogeneity. The grounded mixture of various compositions was shifted into a porcelain crucible and liquefied by heating in a muffle furnace at 1200 ^oC about 90 min. Then the molten state liquid compound was decanted on the mould of brass and afterwards annealed at a temperature of 350 ^oC for 15 hrs to eliminate internal stress to amplify the thermal and mechanical strength of the glass and then the glass specimens were cooled upto room temperature. The transparent and light yellow color of Dy^{3+}-doped BSbMgFSD glasses were obtained and polished to record various optical characterizations. The synthesized glass specimens were categorized as:

a. $70B_2O_3 + 10MgF_2 + 15SrO + 5Sb_2O_3$ (Host: BSbMgFS)
b. $69.9B_2O_3 + 10MgF_2 + 15SrO + 5Sb_2O_3 + 0.1Dy_2O_3$ (BSbMgFSD01)
c. $69.5B_2O_3 + 10MgF_2 + 15SrO + 5Sb_2O_3 + 0.5Dy_2O_3$ (BSbMgFSD05)
d. $69B_2O_3 + 10MgF_2 + 15SrO + 5Sb_2O_3 + 1.0Dy_2O_3$ (BSbMgFSD10)
e. $68.5B_2O_3 + 10MgF_2 + 15SrO + 5Sb_2O_3 + 1.5Dy_2O_3$ (BSbMgFSD15)
f. $68B_2O_3 + 10MgF_2 + 15SrO + 5Sb_2O_3 + 2.0Dy_2O_3$ (BSbMgFSD20)
g. $67.5B_2O_3 + 10MgF_2 + 15SrO + 5Sb_2O_3 + 2.5Dy_2O_3$ (BSbMgFSD25)

II.ii. Characterization Techniques

The structure of the fused glass material (BSbMgFS) without dopant was recorded by Bruker D8 X-ray diffractometer (XRD) glass. Varian Carry-5000 double

beam absorption spectrometer from ultraviolet (UV)-near infrared (NIR) range has been used to measure absorption spectrum of BSbMgFS10 glass matrix. Photoluminescence spectra for all the synthesized matrices were investigated from recorded data by using Edinburg SpectroFluorometer-950 with Xenon (Xe) continuous lamp as an excitation source at a wavelength of 452 nm in between 550-750 nm spectral range. Decay profiles were gained using the said instrument by monitoring the emission wavelength at 575 nm. Refractive index measurement has done from ellipsometer. Above all characterizations have been carried out at room temperature.

III. Results and Discussion

III.i. Physical Properties

The density, refractive index and other physical parameters such as concentration, avg molecular weight, polar radius, interionic distance, field strength, reflection loss, optical dielectric constant, electronic polarizability of BSbMgFSD10 glass matrix were determined [II] and unveiled in Table 1. Smaller field strength shows the larger solubility of RE ion in present glasses. The smaller electronic polarizability makes the glass more stable [XXXIII].

Table 1: Physical properties of BSbMgFSDy10 glass

Physical parameters	BSbMgFSD10
Concentration N($\times 10^{22} ions/cm^3$)	0.144
Avg molecular weight (g/mol)	132.62
Refractive index (n_d)	1.578
Polar radius r_p (Å)	1.65
Density (g/cm^3)	3.17
Inter ionic distance r_i (Å)	4.09
Field strength F ($\times 10^{16}\ cm^2$)	1.06
Dielectric constant Ɛ	1.62
The molar refractivity R_M (cm^3)	7.14
The reflection loss R (%)	0.014
Optical dielectric constant	0.62
The electronic polarizability α_e ($10^{-23}\ cm^3$)	0.28

III.ii. XRD Analysis

X-ray diffraction (XRD) profile of undoped BSbMgFS powder glass sample was measured between 6° to 80° and is presented in Fig-4.1. Broad humps were observed instead of sharp peaks in the XRD profile. These broad humps in XRD pattern were due to unstructured nature of the glass sample. Therefore, the XRD profile confirmed that the structure of the present glass matrix was amorphous.

III.iii. Absorption Spectra

Fig-2 depicts the optical absorption spectrum of 1.0 mol% Dy^{3+}–doped BSbMgFS glass sample in the range of 300–2000 nm. Absorption bands obtained from the $^6H_{15/2}$ ground level to the various excited levels including peak wavelengths, energies and their spectral terms are unvieled in Table-2 [XXXIX]. In the absorption spectrum, couple of weak bands were not observed in the UV-visible region because of absorption edge of host matrix. Among all the transitions, the $^6H_{15/2} \rightarrow {}^6F_{11/2}$ transition centered at 1262 nm is called as hypersensitive transition which agrees the selection rules $\Delta S=0$, $\Delta J=\pm 2$ or $\Delta J \leq 2$ and $\Delta L=\pm 2$ or $\Delta L \leq 2$. This transition is highly sensitive to the host environment around the Dy^{3+} ion [VI, III].

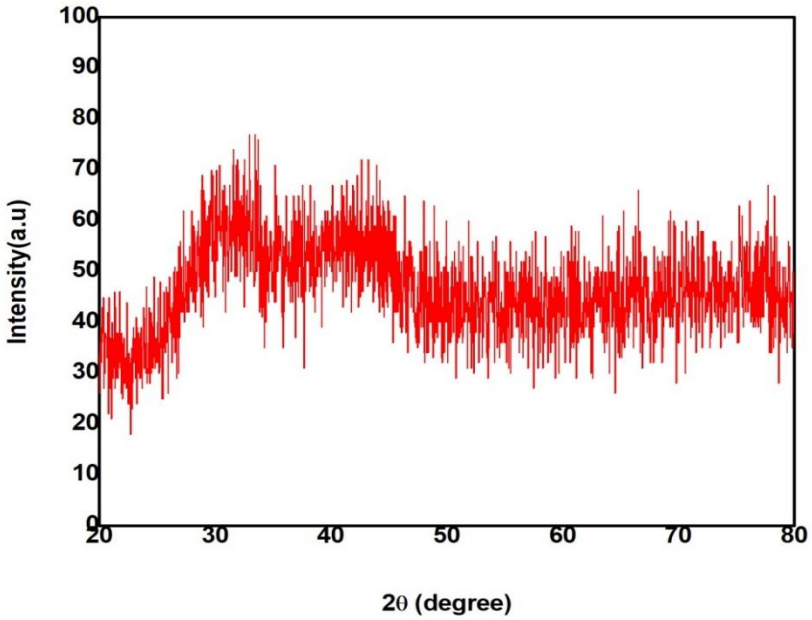

Fig. 1: XRD profile of host glass.

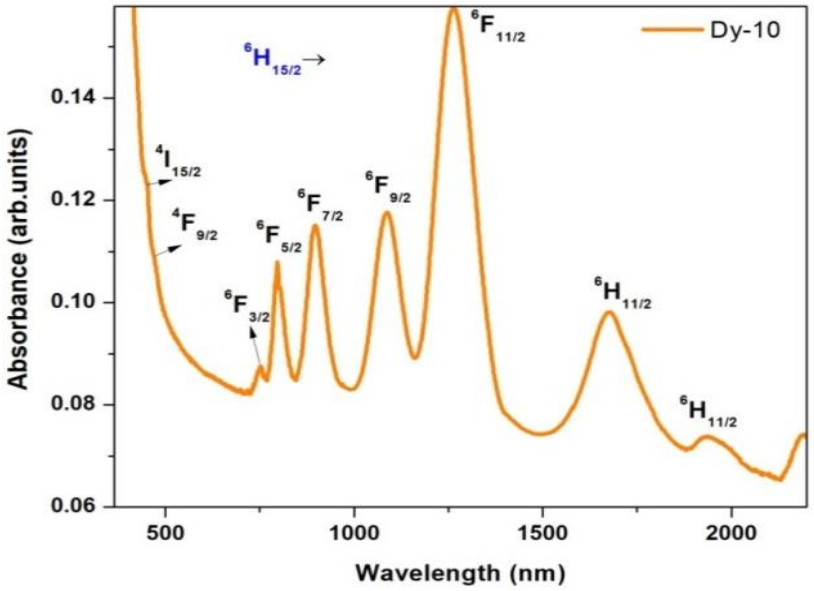

Fig. 2: Absorption spectrum of 1.0 mol% of Dy^{3+}-doped BSbMgFS glass in the visible and near infra-red regions.

$$f_{exp} = 4.32 \times 10^{-9} \int \mathcal{E}(\vartheta) d\vartheta \quad (1)$$

$$f_{cal} = \frac{8\pi^2 mv}{3h(2J+1)} \frac{(n^2+2)^2}{9n} \sum_{\lambda=2,4,6} \Omega_\lambda \, (\Psi J || U^\lambda || \Psi' J')^2 \quad (2)$$

Where $\mathcal{E}(\vartheta)$ is Molar absorptivity of the corresponding energy band of energy ϑ (cm^{-1}), h is the Planck constant, v is frequency, n is refractive index and $\frac{(n^2+2)^2}{9n}$ is called the Lorentz local field correction. The parameter $\left|\left|U^\lambda\right|\right|$ is doubly reduced matrix elements and Ω_λ(λ = 2, 4, 6) are known as JO parameters.

$$\delta_{rms} = \left[\frac{\sum(f_{exp} - f_{cal})^2}{N}\right] \quad (3)$$

Where N = Number of absorption bands.

The intensities of transitions obtained for BSbMgFSDy10 absorption spectra are resolved and expressed in the form of oscillator strengths (f_{exp}, f_{cal}) by using expression in Eq. (1) and Eq. (2). The values of f_{exp} and f_{cal} along with wavelengths, energies of absorption spectra of BSbMgFSDy10 glass are unveiled in Table-2. The smaller δ_{rms} (Eq (3)) shows a significant fit between the values of f_{exp} and f_{cal} and the reliability of J-O theory. A significant study about the rare earth ions bonding (covalency of the RE ion), local structure, symmetrical environment around the RE-ion, viscosity and rigidity of glass can be obtained from the three parameters called as J-O intensity parameters Ω_λ (λ = 2, 4, 6). These are determined by implementing the Judd-Ofelt theory [IV, XI] to evaluated oscillator strengths experimentally. In present work the measured J-O parameters and spectroscopic quality factor (χ) of

BSbMgFSDy01 glass are unfolded along with various published literature [XXXV, XIX, XXVII, XXVXII, XXVI] in Table-3. From the obtained values of Ω_λ (λ = 2, 4, 6), it is observed that the value of Ω_2 is higher than Ω_4 and Ω_6 and follows the trend $\Omega_2 > \Omega_6 > \Omega_4$. The trend confirms the high covalency of Dy^{3+} ion with ligands and more asymmetric environment around the rare earth ion in host [XXXVI, V, VIII, XX].

Table 2: Transition, Peak wavelength (nm), Energy (cm^{-1}), Experimental (f_{exp} x 10^{-6}) and Calculated (f_{cal} x 10^{-6}) oscillator strengths of BSbMgFSD10 glass.

Transition $^6H_{15/2}\rightarrow$	λ_p (nm)	E (cm^{-1})	f_{exp}	f_{cal}	$\lvert\Delta f\rvert$
$^4I_{15/2}$	456	21929	0.033	0.324	0.291
$^4F_{9/2}$	472	21186	0.201	0.123	0.078
$^6F_{3/2}$	753	13280	0.180	0.147	0.33
$^6F_{5/2}$	796	12562	0.875	0.785	0.090
$^6F_{7/2}$	895	11173	1.441	1.601	0.156
$^6F_{9/2}$	1087	9199	1.581	1.555	0.034
$^6F_{11/2}$	1262	7923	3.783	3.791	0.008
$^6H_{11/2}$	1674	5973	0.963	0.900	0.628
$\delta_{rms} = 0.128 \times 10^{-6}$					

Table 3: Judd-Ofelt parameters Ω_λ (λ = 2, 4, 6) (10^{-20} cm^2) and χ (Ω_4/Ω_6) of BSbMgFSD10 glass.

Glass	Ω_2	Ω_4	Ω_6	χ	Trend
BSbMgFSD01	**4.27**	**0.87**	**2.33**	**0.37**	**$\Omega_2 > \Omega_6 > \Omega_4$**
OFBD1.0 [XXXV]	27.9	11.2	0.97	-	$\Omega_2 > \Omega_4 > \Omega_6$
PNABSD10 [XIX]	14.49	1.26	2.23	0.56	$\Omega_2 > \Omega_6 > \Omega_4$
LSPDY10 [XXVII]	6.37	0.34	2.16	0.15	$\Omega_2 > \Omega_6 > \Omega_4$
TBPDy10 [XXV]	7.74	2.31	2.70	0.85	$\Omega_2 > \Omega_6 > \Omega_4$
ZTWDy10 [XII]	6.91	0.99	1.01	0.89	$\Omega_2 > \Omega_6 > \Omega_4$
Glass C [XXVI]	4.89	2.73	3.62	0.75	$\Omega_2 > \Omega_6 > \Omega_4$
Glass D [XXVI]	4.18	1.65	3.03	0.55	$\Omega_2 > \Omega_6 > \Omega_4$

III.iv. Radiative Properties

Table-4 discloses Emission band wavelength (λ_p nm), effective band width ($\Delta\lambda_{eff}$), energy (E cm^{-1}) and the radiative properties such as radiative transition probabilities (A_R) (s^{-1}), branching ratio (β_{exp} & β_{cal}), stimulated emission cross-sections (σ_{se}) ($x10^{-22}$), radiative lifetime τ_R (ms), gain band width $\Delta\lambda_{eff}$ x σ_{se} (x 10^{-28} cm^3) and optical-gain σ_{se} x τ_R (x 10^{-25} s) for the prominent emission transitions concerning to emission spectra of BSbMgFSD01glass matrix under excitation wavelength of 452 nm. The J-O factors Ω_λ (λ = 2, 4, 6) and refractive index were used to estimate the radiative properties by using the following Eq (4), Eq (5), Eq (6), Eq (7), Eq (8), Eq (9) and Eq (10) respectively.

The radiative transition probability A_R is given by

$$A_R(\Psi J, \Psi' J') = \frac{64\pi^4 \nu^3}{3h(2J+1)}\left[\frac{n(n^2+1)}{9} e^2 \sum_{\lambda=2,4,6} \Omega_\lambda \, (\Psi J||U^\lambda||\Psi' J')^2 + n^3 \frac{e^2h^2}{16\pi^2m^2c^2} \, (\Psi J||L + 2S||\Psi' J')^2\right] \quad (4)$$

The sum of the radiative rates $A_R(\Psi J, \Psi' J')$ for each transition gives the total radiative transition (A_T) and is given by

$$A_T(\Psi J, \Psi' J') = \sum_{\Psi J} A_R(\Psi J, \Psi' J') \quad (5)$$

The branching ratio β_R corresponding to the emission transition between higher energy level $\Psi' J'$ to its lower energy level ΨJ can be calculated by

$$\beta_R = \frac{A_R(\Psi J, \Psi' J')}{A_T(\Psi J)} \quad (6)$$

The equation given below relates the A_T with the radiative life time (τ_R),

$$\tau_R = \frac{1}{A_T(\Psi J)} \quad (7)$$

The stimulated emission cross-section (σ_{sm}) between energy levels ΨJ and $\Psi' J'$ is given by

$$\sigma_{sm}(\Psi J, \Psi' J') = \frac{\lambda_p{}^4}{8\pi c n^2 \Delta\lambda_{eff}} A_R(\Psi J, \Psi' J') \quad (8)$$

Where $\lambda_p = Peakwavelengthofthetransitio$

$\Delta\lambda_{eff} = Effectivelinewidth$

$$\text{Gain} = \sigma_{se} \times \tau_{exp} \quad (9)$$

$$\text{Bandwidth} = \sigma_{se} \times FWHM \quad (10)$$

The possibility of stimulated emission in laser media is characterized by branching ratio β_R (β_{exp} & β_{cal}) and for a good laser media it should be greater than or equal to 50%. In the present work branching ratio of $^4F_{9/2} \rightarrow {}^6H_{13/2}$ transition is obtained higher than 50% (0.55). The highest readings of A_R, β_R and σ_{se} are obtained for the transition n $^4F_{9/2} \rightarrow {}^6H_{13/2}$ (yellow).Hence, this can be consider as an appropriate mechanism for

lasing action [X]. Gain band width ($\Delta\lambda_{eff}$ x σ_{se}) and optical-gain (σ_{se} x τ_R) were found to be high for BSbMgFSDy01 and this suggest that BSbMgFSD01 glasses were appropriate for optical amplifier [XX]. A comparison of λ_p, $\Delta\lambda_{eff}$, A_R, β_R and σ_{se} of yellow transition $^4F_{9/2}\rightarrow{}^6H_{13/2}$ for BSbMgFSD01 emission spectra with literature reported for PNABSD [XIX], PKANbDy [XX], DyPPbBi [X], BZABiD05 [XVIII] and ZDTBF [XXVIII] has been presented in Table-4.5

Table 4: Emission band wavelength (λ_p nm), Effective band width ($\Delta\lambda_{eff}$), Energy (cm^{-1}) Radiative transition probabilities (A_R) (s^{-1}), Branching ratio (β_{exp} & β_{cal}), Stimulated emission cross-sections (σ_{se}) ($x10^{-22}$), radiative lifetime τ_R (ms), Gain band width $\Delta\lambda_{eff}$ x σ_{se} (x 10^{-28} cm^3) and Optical-gain (σ_{se} x τ_R x 10^{-25} s) for the prominent emission transitions of BSbMgFSD01glass matrix.

Transition $^4F_{9/2}\rightarrow$	**λ_p**	**E**	**$\Delta\lambda_{eff}$**	**A_R**	**Branching ratio(β_R)**		**σ_{se}**	**$\Delta\lambda_{eff}$ x σ_{se}**	**σ_{se} x τ_R**
					β_{exp}	**β_{cal}**			
$^6H_{15/2}$	480	20796	17.42	95	0.15	0.23	2.3	4.0	5.71
$^6H_{13/2}$	**573**	**17429**	**18.92**	**262**	**0.49**	**0.55**	**13.7**	**25.9**	**32.61**
$^6H_{11/2}$	663	15060	16.91	63	0.14	0.18	5.30	8.96	21.32
τ_R = 2.38									

Table 5: Emission band wavelength (λ_p nm), energy (E cm^{-1}), Effective band width ($\Delta\lambda_{eff}$), radiative transition probabilities (A_R) (s^{-1}), branching ratio (β_{exp} & β_{cal}), Stimulated emission cross-sections (σ_{se}) ($x10^{-22}$) and radiative lifetime τ_R (ms) for $^4F_{9/2}\rightarrow{}^6H_{13/2}$ level of BSbMgFSD01 glass matrix with various Dy^{3+}-doped glasses.

Glass	**λ_p**	**E**	**$\Delta\lambda_{eff}$**	**A_R**	**Branching ratio**		**σ_{se}**
					β_{exp}	**β_{cal}**	
BSbMgFSDy01	**573**	**17429**	**18.92**	**262**	**0.49**	**0.55**	**13.7**
PNABSD[XIX]	575	17391	17.19	955	0.71	0.77	2.92
PKANbDy[XX]	575	17391	18.59	2245	0.55	0.72	6.40
DyPPbBi[X]	573	17429	14.3	1135	-	0.66	3.88
BZABiD05[XVIII]	577	17331	15.25	1225	0.47	0.62	36.25
ZDTBF[XXVIII]	574	17421	7.220	539	0.46	0.51	6.01

III.v. CIE Chromaticity Diagram: Representation of Coordinates

The feasibility of BSbMgFSD glasses for white light emission has been inspected from the well-known chromaticity diagram (CIE 1931) [XXXVII]. The tristimulus values of X, Y and Z are utilized in below equations to assess the color coordinates (x, y and z).

$$x = \frac{X}{X+Y+Z} \tag{11}$$

$$y = \frac{Y}{X+Y+Z} \tag{12}$$

$$z = \frac{Z}{X+Y+Z} \tag{13}$$

The color coordinates (x, y) are shown in Fig. 4.6 and also represented in Table 6. With increase of Dy^{3+} concentration color coordinates (x, y) of BSbMgFSDy01 glass were seemed close to the white region and moved to yellowish-white region upon 452nm excitation. This specifies that the examined BSbMgFSD glasses could be a suitable candidate for white emission applications.

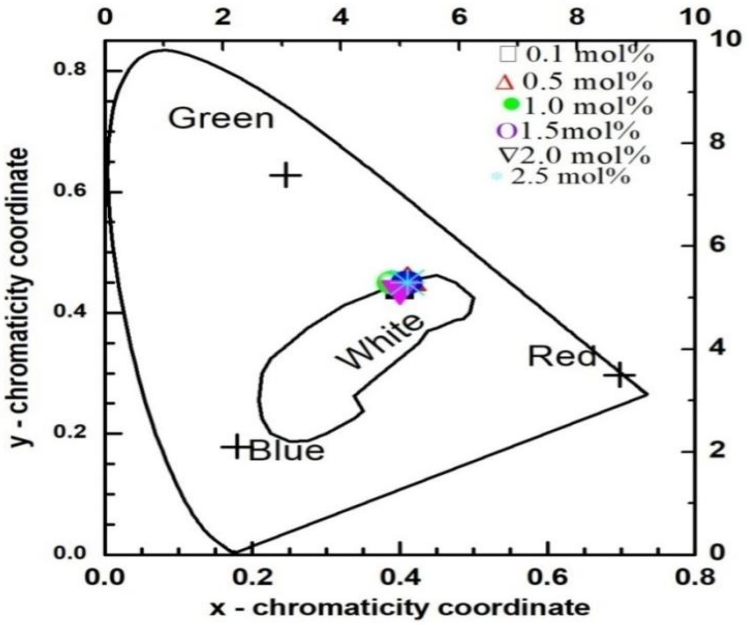

Fig. 6: Representation of chromaticity coordinates of Dy^{3+}-doped BSbMgFS glasses in CIE chromatic diagram.

Table 6: Chromaticity coordinates (x, y) and Y/B ratio of BSbMgFSD system.

Glass	X	Y	Y/B	References
BSbMgFSDyy01	0.40	0.44	2.38	[Present work]
BSbMgFSDy05	0.41	0.45	2.74	"
BSbMgFSDy10	0.38	0.43	2.06	"
BSbMgFSDy15	0.41	0.45	2.81	"
BSbMgFSDy20	0.40	0.44	2.63	"
BSbMgFSDy25	0.41	0.45	2.43	"
BWZnLiNaDy(f)	0.42	0.45	2.98	[XXIX]
SLBiBDy10	0.43	0.44	0.98	[XXIV]
BPB01D	0.39	0.45	2.67	[IX]
BPB05D	0.39	0.44	2.46	[IX]

IV. Conclusions

In the current study the conventional melt-quenching technique has been employed for synthesizing the dysprosium (Dy^{3+}) doped antimony-magnesium-strontium-oxyfluoroborate (BSbMgFSD) glasses and investigated for white light generation and potential laser applications. The amorphous nature of these glasses has been confirmed from recorded XRD. The calculations of J-O intensity parameters Ω_λ (λ = 2, 4, 6) for BSbMgFSD10 have been completed from the values of f_{exp} and f_{cal}. Higher value of Ω_2 showed high covalency in the vicinity of Dy^{3+} ion in the present glass system. An intense emission band was observed at 575 nm under 425 nm excitation wavelengths which corresponds to the $^4F_{9/2} \rightarrow {}^6H_{13/2}$ (Yellow) transition of Dy^{3+} ion. The radiative properties like branching ratio, transition probability and stimulated emission cross section the transition $F_{9/2} \rightarrow {}^6H_{13/2}$ in BSbMgFSD01 was observed to be high and this suggests that the BSbMgFSD01 glasses are suitable for yellow laser emission. Results obtained from CIE1931 propose that the 0.5 mol% Dy^{3+}-doped BSbMgFS glass could be suitable candidate for white light emitting devices and lasers applications in the visible region at 575 nm upon excitation of 425 nm.

References:

I. A. Lira, A. Speghini, E. Camarillo, M. Bettinelli, U. Caldino, Spectroscopic evaluation of Zn (Po_3): Dy^{3+} glass as active medium of solid state laser, Opt. Mater. 38 (2014) 188.

II. A.S. Rao, Y.N. Ahammed, R.R. Reddy, T.V.R. Rao, Spectroscopic studies of Nd^{3+}-doped alkali fluoroborophosphate glasses, Opt. Mater. 10 (1998) 245–252.

III. A. Thulasiramudu, S. Buddhudu, Optical characterization of Sm^{3+} and Dy^{3+} doped ZnO-PbO-B_2O_3 glasses, Spectrochim Acta Part A. 67 (2007) 802-807.

IV. B. R. Judd, Optical absorption intensities of rare earth ions, Phys. Rev. 127 (1962) 750.

V. C. Gorller-Walrand, K. Binnemans, Handbook on the Physics and Chemistry of Rare Earths, Spectral Intensities of f-f Transitions, vol. 5, Elsevier/North-Holand, Amsterdam, 1998, 101-264.

VI. C.K. Jorgenson, B.R. Judd, Hypersensitive pseudoquadrapole transition in Lanthanides, Mol. Phys. 8 (1964) 281–290.

VII. C. Nageswara Raju, S.Sailaja, S. Hemasundara Raju, S.J.Dhoble, U.Rambabu, Young-Dahl Jho, B.Sudhakar Reddy, Emission analysis of CdO–Bi_2O_3–B_2O_3 glasses doped with Eu^{3+} and Tb^{3+},Ceramic.International 40(2014) 7701–7709.

VIII. D.K. Sardar, W.M. Bradly, R.M. Yow, J.B. Gruber, B. Zandi, J. of Luminescence 106 (2004) 195-203.

IX. D. Rajesh, Y.C. Ratnakaram, M. Seshadri, A. Balakrishna, T. Satya Krishna, Structural and luminescence properties of Dy^{3+} ion in strontium lithium bismuth borate glasses J. Lumin. 132 (2012) 841-849.

X. G. Chinna Ram, T. Narendrudu, S. Suresh, A. Suneel Kumar, M.V. Sambasiva Rao, V. Ravi Kumar, D. Krishna Rao, Investigation of luminescence and laser transition of Dy^{3+}ion in P_2O_5-PbO-Bi_2O_3 -Dy_2O_3 glasses, Optical Materials 66 (2017) 189-196.

XI. G. S. Ofelt, Intensities of crystal spectra of rare earth ions, J. Chem. Phys. 37 (1962) 511.

XII. G. Venkata Rao, C.K. Jayasankar., "Dy^{3+}-doped tellurite based tungsten zirconium glasses: Spectroscopy study", J. Mol. Struct. 1084 (2015) 182-189.

XIII. H.A. Othman, G.M. Arzumanyan, D. Moncke, The effect of alkaline earth oxides and cerium concentration on the spectroscopic properties of Sm/Ce doped lithium alumino-phosphate glasses Opt. Mater. 62 (2016) 689–696.

XIV. J. Juarez-Batalla, A.N. Meza-Rocha, G.Munoz, H.I.Camarillo, U.Caldino, Luminescence properties of Tb^{3+}-doped zinc phosphate glasses for green laser application, Opt Mater. 58(2016) 406–411.

XV. Kenyon A.J, "Recent developments in rare-earth doped materials for optoelectronics, Prog. J. Quantum Electron, 26(2002) 225–284.

XVI. K. Jaroszewski, P. Głuchowski, M. Chrunik, R. Jastrz, A. Majchrowski, D. Kasprowicz, Near-infrared luminescence of $Bi_2ZnOB_2O_6$:Nd^{3+}/PMMA composite, Optical Materials 75 (2018) 13-18.

XVII. K.S.V. Sudhakar, M. Srinivasa Reddy, L. Srinivasa Rao, N. Veeraiah, Influence of modifier oxide on spectroscopic and thermoluminescence characteristics of Sm^{3+} ion in antimony borate glass system, J. of Luminescence 128 (2008) 1791– 1798.

XVIII. K. Swapna, Sk. Mahamuda, A. Srinivasa Rao, M. Jayasimhadri, T. Sasikala, L. Rama Moorthy, Optical absorption and luminescence characteristics of Dy^{3+} doped Zinc Alumino Bismuth Borate glasses for lasing materials and white LEDs, Journal of Luminescence 139 (2013) 119 -124.

XIX. K. Vijaya Babu, Sandhya Cole, Luminescence properties of Dy^{3+}-doped alkali lead alumino borosilicate glasses, Ceramics International (2018) 9080-9090.

XX. K.V. Krishnaiah, K. Upendra Kumar, C.K. Jayasankar, Mater. Exp. 3 (2013) 61-70.

XXI. L. Eyring (Ed.), Progress in the Science and Technology of the Rare Earths, Pergamon, London (1966).

XXII. M.J. Plodinec, Borosilicate glass for nuclear waste immobilisation, Glass Technol. 41(2000), 186-192.

XXIII. M. Kemere, J. Sperga, U. Rogulis, G. Krieke, J. Grube, Structural and optical studies on Sm^{3+} ions doped bismuth fluoroborate glasses for visible laser applications, J. Lumin. 181 (2017) 25–30.

XXIV. M. Sundara Rao, V. Sudarsan, M.G. Brik, Y. Gandhi, K. Bhargavi, M. Piasecki, I.V. Kityk, N. Veeraiah, De-quenching influence of aluminum ions on Y/B ratio of Dy^{3+} ions in lead silicate glass matrix, Journal of Alloys and Compounds 575 (2013) 375-381.

XXV. M.V. Vijaya Kumar, B.C. Jamalaiah, K. Rama Gopal, R.R. Reddy., "Optical absorption and fluorescence studies of Dy^{3+}-doped lead telluroborate glasses", J. Lumin. 132 (2012) 86-90.

XXVI. Nisha Deopa, A.S. Rao, Photoluminescence and energy transfer studies of Dy^{3+} ions doped lithium lead alumino borate glasses for w-LED and laser applications, J. of Luminescence 192 (2017) 832–841.

XXVII. N. Kiran, A. Suresh Kumar., "White light emission from Dy^{3+} doped sodium lead borophosphate glasses under UV light excitation", J. Mol. Struct. 1054 (2013) 6-11.

XXVIII. P. Suthanthirakumar, K. Marimuthu, Investigations on spectroscopic properties of Dy^{3+} doped zinc telluro-fluoroborate glasses for laser and white LED application, J. Mol. Struct. 1125 (2011) 443-452.

XXIX. R.C. Lucacel, I. Ardelean, FT-IR and Raman study of silver lead borate-based glasses, J. Non-Cryst. Solids. 353 (2007) 2020-2024.

XXX. S. Abed, H. Boughrraf, K. Bouchouit, Z. Sofiani, B. Derkowska, M.S. Aida, B. Sahraoui, Influence of Bi doping on the electrical and optical properties of ZnO thin films, Superlattice Microstruct. 85 (2015) 370-378.

XXXI. S.D. Jackson, Continuous wave 2.9μm dysprosium-doped fluoride fiber laser, Appl. Phys. Lett. 83 (2003) 1316-1318.

XXXII. S. Gai, C. Li, P. Yang, J. Lin, Recent progress in rare earth micro/nanocrystals: soft chemical synthesis, luminescent properties, and biomedical applications, Chem. Rev. 114 (2014) 2343-2389.

XXXIII. Sk. Mahamuda, K. Swapna, P. Packiyaraj, A. Srinivasa Rao, G. Vijaya Prakash, Lasing potentialities and white light generation capabilities of Dy^{3+} doped oxyfluoro borate glasses, J.Lumin. 153 (2014) 382−392.

XXXIV. Sudhakar Reddy: Judd–Ofelt theory: optical absorption and NIR emission spectral studies of Nd^{3+}: CdO–Bi_2O_3– B_2O glasses for laser applications, J Mater Sci. 47 (2012) 772–778.

XXXV. Swapna K, Mahamuda S, Rao AS, Jayasimhadri M, Moorthy LR. Visible fluorescence Characteristics of Dy^{3+} doped zinc alumino bismuth borate glasses for optoelectronic devices, Ceramic Int. 39 (2013) 8459–65.

XXXVI. T. Srihari, C.K. Jayasankar, Fluorescence properties and white light generation from Dy^{3+}-doped niobium phosphate glasses, Optical Materials 69 (2017) 87-95.

XXXVII. Valluri Ravi Kumar, G. Giridhar, N. Veeraiah, Influence of modifier oxide on emission features of Dy3+ ion in Pb3O4 –ZnO–P2O5 glasses, Optical Materials, 60 (2016) 594-600.

XXXVIII. W. Bi, N. Louvain, N. Mercier, J. Luc, I. Rau, B. Sahraoui, A switchable NLO organic- inorganic compound based on conformationally chiral disulfide molecules and Bi(III)I5 iodobismuthate networks, Adv. Mater. 20 (2008) 1013-1017.

XXXIX. W.T. Carnall, P.R. Fields, K.Rajnak, Electronic Energy Levels in the Trivalent Lanthanide AquoIons. I. Pr^{3+}, Nd^{3+}, Pm^{3+}, Sm^{3+}, Dy^{3+}, Ho^{3+}, Er^{3+}, and Tm^{3+}, J. Chem. Phys. 49 (1968) 4424–4442.